Nuclear Instruments and Methods in Physics Research B 326 (2014) 117–120

Contents lists available at ScienceDirect

Nuclear Instruments and Methods in Physics Research B

journal homepage: www.elsevier.com/locate/nimb

The shape of ion tracks in natural apatite

D. Schauries [a,*], B. Afra [a], T. Bierschenk [a], M. Lang [b], M.D. Rodriguez [a], C. Trautmann [c,d], W. Li [b], R.C. Ewing [b], P. Kluth [a]

[a] Department of Electronic Materials Engineering, Research School of Physics and Engineering, The Australian National University, Canberra, ACT 0200, Australia
[b] Department of Earth and Environmental Sciences, University of Michigan, Ann Arbor, MI 48109, USA
[c] GSI Helmholtz Centre for Heavy Ion Research, Planckstrasse 1, 64291 Darmstadt, Germany
[d] Technische Universität Darmstadt, 64287 Darmstadt, Germany

ARTICLE INFO

Article history:
Received 1 July 2013
Received in revised form 27 October 2013
Accepted 27 October 2013
Available online 30 January 2014

Keywords:
Ion irradiation
Ion tracks
SAXS
Apatite

ABSTRACT

Small angle X-ray scattering measurements were performed on natural apatite of different thickness irradiated with 2.2 GeV Au swift heavy ions. The evolution of the track radius along the full ion track length was estimated by considering the electronic energy loss and the velocity of the ions. The shape of the track is nearly cylindrical, slightly widening with a maximum diameter approximately 30 μm before the ions come to rest, followed by a rapid narrowing towards the end within a cigar-like contour. Measurements of average ion track radii in samples of different thicknesses, i.e. containing different sections of the tracks are in good agreement with the shape estimate.

1. Introduction

In many materials, swift heavy ions create long narrow defect structures along their trajectory. These so-called ion tracks are generally only a few nanometres in diameter and depending on the kinetic energy of the ions can reach lengths of up to tens of micrometres. Based on their extremely large aspect ratio, ion tracks are suitable for a wide range of applications in materials science, nanotechnology, biophysics, geo- and thermochronology, archaeology, and interplanetary science. In nature, ion tracks are produced when radioactive trace amounts such as thorium or uranium fission into two fragments of about 1 MeV per nucleon kinetic energy. In minerals containing fissile impurities such as apatite or zircon, tracks of fission fragments are used for dating and constraining the thermal history of geological samples [1].

The track formation process and the resulting track cross-sections are intimately related to the ion energy or more specifically the electronic energy loss of the ion when travelling through the material. As the energy decreases when the ion traverses the material, the cross-section of these tracks varies more or less over the entire track length, giving the tracks a distinct shape. Measurements of the shape of the tracks are extremely difficult as most techniques are insensitive to the small variation in the track size over its depth. Only recently, time-consuming transmission electron microscopy (TEM) measurements have revealed the shape of individual tracks along the trajectory of 80 MeV ^{129}Xe ions in apatite [2].

By means of synchrotron-based small angle X-ray scattering (SAXS), we have previously analysed ion tracks in many different materials including apatite [3–5]. Track radii deduced from SAXS measurements represent values averaged over the entire track length. In this work, we address the fact that the track radius changes with energy loss and provide an estimate of the resulting track shape. Therefore, apatite samples of different thickness (containing only parts or the entire track) were irradiated with a range of ions of different energies. By SAXS analysis of the different track sections and considering the respective energy loss, a cigar-like track shape is suggested for high energy ion irradiation.

2. Experimental

Crystalline fluorapatite [$Ca_{10}(PO_4)_6F_2$] from Durango, Mexico, was annealed at 500 °C for 24 h to remove existing fission tracks and other defects in the specimen. One of the samples was polished down to a thickness of 110 μm and irradiated with 100 MeV ^{127}I ions to a fluence of 5×10^{10} ions/cm^2 at the Heavy Ion Accelerator Facility of the Australian National University (Canberra). The beam energy and ion mass is similar to that of natural fission fragments. The incident ion direction was kept normal to the polished surface. In a similar manner, 20, 30, 57, 80 and

* Corresponding author. Tel.: +61 2 612 50371
E-mail address: daniel.schauries@anu.edu.au (D. Schauries).

0168-583X/$ - see front matter © 2014 Elsevier B.V. All rights reserved.
http://dx.doi.org/10.1016/j.nimb.2013.10.071

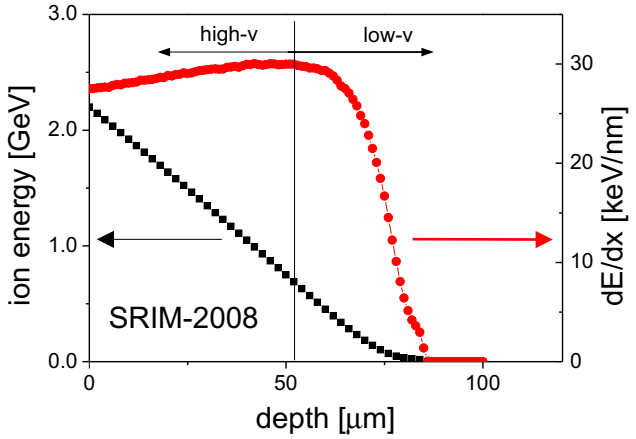

Fig. 1. SRIM calculation showing the evolution of the ion energy (circles) and electronic energy loss (squares) of 2.2 GeV Au ions while penetrating through apatite.

200 ± 3 μm thick samples were irradiated with 2.2 GeV ^{197}Au ions at the GSI Helmholtz Centre for Heavy Ion Research (Darmstadt, Germany). For all irraditions, a fluence of 5×10^{10} ions/cm^2 was applied and the incident beam direction was normal to the polished sample surface. Samples were irradiated in three different beamtimes.

The energy loss and projected range of 2.2 GeV Au ions in apatite was calculated with the SRIM-2008 code [6] assuming a mass density of 3.2 g/cm^3. The evolution of the kinetic energy and electronic energy loss as a function of penetration depth is shown in Fig. 1. The energy steadily decreases until the ion comes to rest at a depth of about 86 μm. According to [7], the threshold for track formation is 2 keV/nm, thus no tracks form on the last μm where dE/dx falls below this critical value. The electronic energy loss initially increases by about 10% and reaches the Bragg maximum at a depth of about 52 μm. From this point on, the energy loss decreases rapidly towards the end of the ion path. We note, that values calculated by SRIM typically include an uncertainty of about 10% [8]. As the track diameter depends on dE/dx_{el}, it can be expected that the track size continuously changes over its full range.

SAXS measurements were carried out at the SAXS/WAXS beamline at the Australian Synchrotron (Melbourne, Australia) using an X-ray energy of 11 keV and a camera length of 1580 mm. The sample tilt was adjusted such that incident X-ray beam and ion track comprise an angle of typically 10°. Spectra were collected using a Pilatus 1 M detector with exposure times of 5 and 10 s. An unirradiated sample provided data for background removal. Detailed overview for SAXS measurements of ion tracks are discussed in references [3–5].

3. Results and discussion

Fig. 2(a) shows the X-ray scattering intensity for apatite irradiated with 100 MeV ^{127}I ions (0.8 MeV/u) as a function of the scattering vector q. The irradiation with this combination of ion and energy is particularly interesting, as these ions are of similar mass and energy as natural ^{238}U fission products [1]. The best fit to the SAXS spectrum was found modelling the tracks as cylinders with a constant density difference, $\Delta\rho_0$ between track and matrix material. The corresponding form factor can be expressed as

$$f(q) = (2\pi LR\Delta\rho_0/q)\,J_1(Rq) \quad (1)$$

where L is the track length, R the track radius, and J_1 the first order Bessel function [3]. The scattering intensity is given by $I(q) \sim |f(q)|^2$.

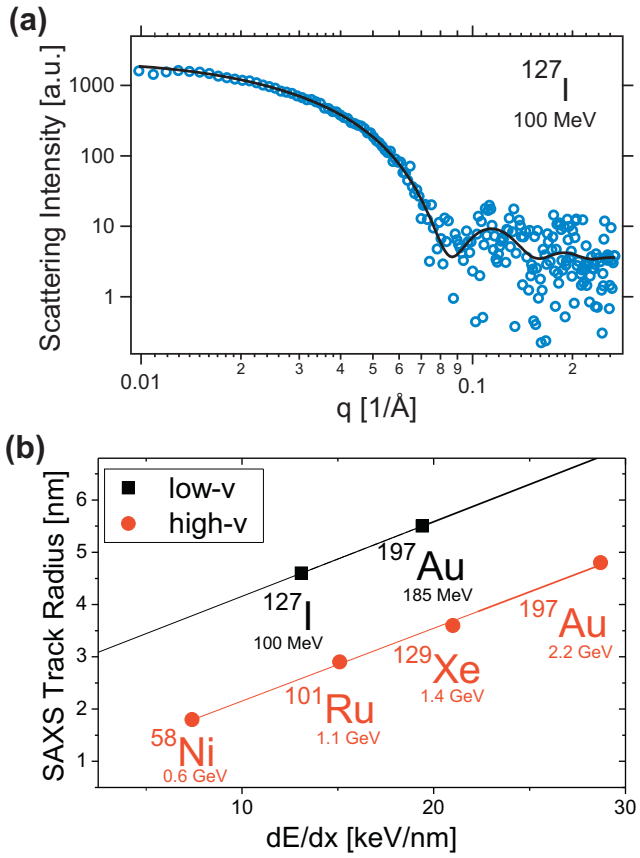

Fig. 2. (a) SAXS intensity from ion tracks in apatite irradiated with 100 MeV I ions (symbols). The hard cylinder fit (line) reports an average radius of 4.5 ± 0.2 nm. (b) Average radius as a function of electronic energy loss in apatite for a range of low (squares) and high velocity (circles) irradiation conditions.

To account for the variation of the radius over the track length, the radius is convoluted with a narrow Gaussian distribution of width σ_r [4,9]. The best fitting parameters were determined iteratively by a least squares algorithm. The fit in Fig. 2(a) yields an average radius of 4.5 ± 0.2 nm. A track length of 10 μm was estimated from SRIM-2008 calculations, using the same methodology as for the 2.2 GeV Au irradiated samples. Both are consistent with measurements of natural fission tracks in apatite, where typically radii between 2.5 and 5.0 nm and track lengths between 10 and 20 μm are reported [10].

The irradiation of apatite with 100 MeV I ions (0.8 MeV/u) complements previous irradiation experiments with 0.9 MeV/u Au (low velocity) [5] and a variety (Ni, Ru, Xe, Au) of 11.1 MeV/u ions (high velocity) [3]. Calculating the average ion track radii determined from SAXS measurements are shown as a function of their average electronic energy loss in Fig. 2(b). We note that SAXS provides a measure of the average volume weighted track radius over the sample depths. The average energy loss for each ion is straight forward for high velocity irradiation: All 2.2 GeV Au-irradiated samples were kept much thinner (30–40 μm) than the track length of 72–85 μm such that the variation of the electronic energy loss does not exceed 5%. As this variation is small, the track volume weighted average energy loss corresponding to the radius measured by SAXS can be approximated by the simple average of dE/dx_{el} over the sample thickness.

In contrast, tracks produced by low velocity ions are much shorter (10–14 μm) and of conical shape as revealed by TEM measurements [2]. On the low energy side of the Bragg maximum, the energy loss strongly varies along the ion path before the projectile comes to rest (see Fig. 1). Here, the average energy loss is

considered to be the value at the depth where the cone-shaped track has equal volume parts. Fig. 2(b) shows that the track radii increase linearly as a function of the average energy loss. For a given energy loss, the radii of tracks produced by low velocity ions are approximately 2.0 nm larger than those of high velocity ions. This difference is ascribed to the velocity effect which is based on the fact that the higher the ion velocity the larger is the created electron cascade. The deposited energy is thus spread out into a larger volume leading to a lower deposited energy density. This effect explains the smaller track radii at higher beam velocities [11,12]. The track shape is therefore not only governed by the energy loss along the ion path but also to a large extent by the ion velocity.

To reconstruct the shape of the full track, the track radius in the high-energy (above the Bragg-peak, energy $>$ 800 MeV) and low-energy sections (below the Bragg peak, energy $<$ 800 MeV) of the ion trajectory were deduced from the two data sets in Fig. 2(b) by separately interpolating the respective radius-versus-dE/dx curves, as they strongly imply a linear relationship. Fig. 3 shows that the track (circles) in the high-velocity regime (Section 0–52 μm) the radius is initially 30% larger than on the surface and then decreases rapidly towards the track end to approximately half the size. To connect the two velocity regimes, the radius curve was smoothen by linear interpolation (squares) illustrating the cigar-like track shape. An exposure of ion tracks in apatite to elevated temperatures leads to recrystallization of the damaged material, an effect that is greatly enhanced at the narrow track end thus leading to shortening of the track [13]. This may cause an observed small, but measureable, increase in average track radius at the onset of track annealing [14].

As previously demonstrated, SAXS provides a measure of the average track radii in apatite with very high precision. Fig. 4 shows the scattering intensity for apatite samples of different thicknesses irradiated with 2.2 GeV Au ions. The analysis was performed as outlined above for the 100 MeV I irradiated sample. The uncertainty for each track radius is estimated to 1% consistent with our previous studies [3,14]. The sample thicknesses are marked by vertical lines in Fig. 3 and indicate the parts of the track that are contained in the sample. For the thin samples (20, 30 μm) average track radii of 4.86 and 4.87 ± 0.05 nm were measured. The thicker samples (57, 80 and 200 μm) show a radius between 5.01 and 5.04 ± 0.05 nm, an increase of 3–4% over the thin samples. The polydispersity for the average radii increases from

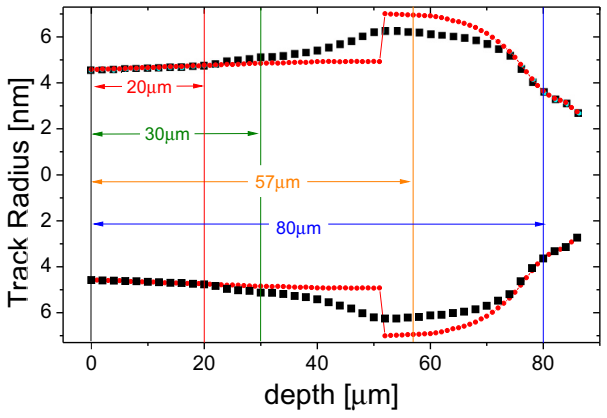

Fig. 3. Calculation of the shape of an ion track in apatite from irradiation with 2.2 GeV Au ions. For visualisation purposes the radius has been mirrored. From the surface to a depth of 52 μm, the radius was calculated by the high velocity (high-v) approximation while for greater depth the low velocity (low-v) model was used (circles). The squares show the result of linear interpolation and the estimated track shape (data point density has been reduced for enhanced readability). Samples of different thicknesses are displayed with arrows.

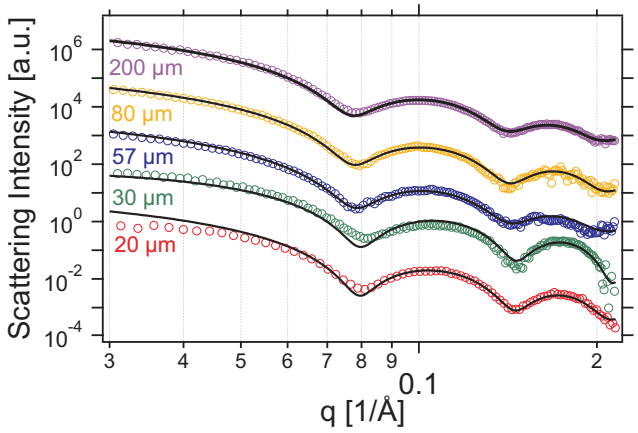

Fig. 4. SAXS scattering intensity of ion tracks in apatite with different thicknesses (symbols). A hard cylinder model was used to fit the results (solid lines).

Table 1
Track radius and polydispersity for apatite samples of different thickness as measured with SAXS and the corresponding average radius, calculated via the track shape. All samples were irradiated with 2.2 GeV Au ions.

Thickness (μm)	SAXS track radius (nm)	SAXS radius polydispersity (nm)	Calculated average radius (nm)
20	4.81 ± 0.05	0.26 ± 0.05	4.7
30	4.87 ± 0.05	0.31 ± 0.05	4.8
57	5.03 ± 0.05	0.38 ± 0.05	5.2
80	5.01 ± 0.05	0.48 ± 0.05	5.3
200	5.04 ± 0.05	0.37 ± 0.05	5.2

0.25 ± 0.05 nm for thin to 0.48 ± 0.05 nm for thick samples, reflecting the larger variations in the track cross-sections in the thicker samples as they contain longer sections of the tracks. The fitting parameters are listed in Table 1 together with the estimates of the calculated average track radii R_{ave} from Fig. 3. These values were calculated by integrating the radius $R(x)$ over the respective sample thickness L via:

$$R_{ave}^2 \pi L = V_{ave} = \int_0^L R^2(x)\pi dx \quad (2)$$

As a result of the linear extrapolation of the track radius (see Fig. 2b), the results only have an uncertainty within two significant figures. The calculated results show comparable radii for the thin samples, although their absolute value is slightly underestimated. They correctly predict an increase towards thicker samples due to the largest cross-section being present around a depth of 55 ± 5 μm. We note that the samples originate from three different ion irradiation beamtimes, although all parameters were kept as identical as possible. This shows the reproducibility and consistency of the observed track formation as well as the reliability of the SAXS measurements.

4. Conclusion

A combination of track data from irradiations with low and high velocity ion and electronic energy loss calculations was used to estimate the shape of ion tracks resulting from high energy ion irradiation in apatite. The results agree with the average track radii measured with SAXS of apatites of several thicknesses containing ion tracks that contain different sections of the whole track. The variation of the average track radius, even though as small as only 3–4%, was resolvable with SAXS. The radius increases in the first half of the ion track length and reaches its maximum within the

final 30 μm of the ion range. After this maximum the radius decreases rapidly and eventually drops to zero. This shape is different from that of low energy (low velocity) ions, for which there is typically a rapid decrease in track size from the beginning [2].

Acknowledgments

This research was undertaken on the SAXS/WAXS beamline at the Australian Synchrotron. P.K. acknowledges the Australian Research Council for financial support. R.C.E and M.L. acknowledge the support of the Office of Basic Energy Sciences of the USDOE (DE-FG02–97ER45656).

References

[1] G. A. Wagner and P. Van den Haute, Fission-Track Dating, Kluwer Academic Publishers, 1992.
[2] W.X. Li, M. Lang, A.J.W. Gleadow, M.V. Zdorovets, R.C. Ewing, Earth Planet. Sci. Lett. 321 (2012) 121–127.
[3] B. Afra, M. Lang, M.D. Rodriguez, J. Zhang, R. Giulian, N. Kirby, R.C. Ewing, C. Trautmann, M. Toulemonde, P. Kluth, Phys. Rev. B 83 (2011) 064116–064120.
[4] P. Kluth, C.S. Schnohr, O.H. Pakarinen, F. Djurabekova, D.J. Sprouster, R. Giulian, M.C. Ridgway, A.P. Byrne, C. Trautmann, D.J. Cookson, K. Nordlund, M. Toulemonde, Phys. Rev. Lett. 101 (2008) 175503–175506.
[5] B. Afra, M.D. Rodriguez, M. Lang, R.C. Ewing, N. Kirby, C. Trautmann, P. Kluth, Nucl. Instr. Meth. Phys. Res. B 286 (2012) 243–246.
[6] J.F. Ziegler, J.P. Biersack, U. Littmark, The Stopping and Range of Ions in Matter, Pergamon, New York, 1985.
[7] R. Tisserand et al., Nucl. Instr. Meth. Phys. Res. B 215 (2004) 129–136.
[8] J.F. Ziegler, M.D. Ziegler, J.P. Biersack, Nucl. Instr. Meth. Phys. Res. B 268 (2010) 1818–1823.
[9] M.D. Rodriguez, B. Afra, C. Trautmann, M. Toulemonde, T. Bierschenk, J. Leslie, R. Giulian, N. Kirby, P. Kluth, J. Non-Cryst. Solids 358 (2012) 571–576.
[10] R.C. Jonckheere, G.A. Wagner, Am. Mineral. 85 (2000) 1744–1753.
[11] A. Meftah, F. Brisard, J.M. Costantini, M. Hage-Ali, J.P. Stoquert, F. Studer, M. Toulemonde, Phys. Rev. B 48 (1993) 920–925.
[12] S. Klaumünzer, Nucl. Instr. Meth. Phys. Res. B 225 (2004) 136–153.
[13] W. Li, L. Wang, M. Lang, C. Trautmann, R.C. Ewing, Earth Planet. Sci. Lett. 302 (2011) 227–235.
[14] D. Schauries, M. Lang, O.H. Pakarinen, S. Botis, B. Afra, M.D. Rodriguez, F. Djurabekova, K. Nordlund, D. Severin, M. Bender, W.X. Li, C. Trautmann, R.C. Ewing, N. Kirby, P. Kluth, J. Appl. Cryst. 46 (2013) 1558–1563.